Focus on Fluids journals.cambridge.org/focus

Droplets in turbulence: a new perspective

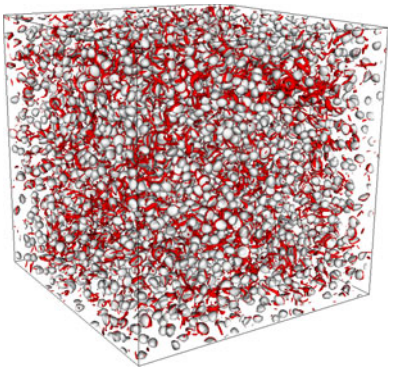

Martin R. Maxey†

Division of Applied Mathematics, Brown University, Providence RI, 02912, USA

Stirring olive oil and vinegar to make salad dressing creates an emulsion of vinegar droplets in oil. More vigorous stirring gives smaller droplets, while if left to sit the droplets will begin to coalesce and the two fluids will separate. In this vein, Dodd & Ferrante (*J. Fluid Mech.*, vol. 806, 2016, pp. 356–412) present a new analysis of how homogeneous turbulence in a carrier fluid interacts with a suspension of droplets of an immiscible liquid. Based on a set of direct numerical simulations, the authors provide new insights on how turbulence affects the motion of the droplets, their shape and size; then in turn how the droplets alter the flow including effects of interfacial surface energy on the kinetic energy of the flow.

Key words: multiphase flow, multiphase and particle-laden flows

1. Introduction

Much of the recent work on dispersed two-phase turbulence has focused on solid particles in a gas or liquid flow. The questions asked relate to how the turbulence causes particles to disperse or interact with each other and how the turbulence itself may be modified by their presence. Key parameters are the density ratio of the solid to the carrier fluid, $\varphi = \rho_d/\rho_c$, and the volume fraction that the particles occupy, ϕ_v. Even if ϕ_v is low, a substantial portion of the total kinetic energy can reside in the particle phase if the particles are denser than the carrier fluid. Such particles are inertial and there is a lag in their response to changes in the surrounding flow that leads not only to a net slip in the velocity between the two phases but also to an inertial bias where the particles tend to accumulate in regions of high strain rate or low vorticity in the flow (Balachandar & Eaton 2010). So even if the particles are initially randomly dispersed they can develop clusters at scales larger than the particle size which in turn can have a dynamic effect back on the turbulence. Whether it a jet flow, a boundary layer flow or convection in an atmospheric cloud, there is a large length scale L that

† Email address for correspondence: martin_maxey@brown.edu

doi:10.1017/jfm.2017.96

characterizes the energetic forcing of the turbulence and then a continuous spectrum of scales down to the smallest Kolmogorov length scale η_K associated with the eventual dissipation of kinetic energy by viscous forces. The smallest particles with diameter $D \leqslant \eta_K$ enhance the viscous dissipation range of the turbulence. Larger particles can inject energy at a length scale comparable to D. This is associated with a local wake flow and disturbance the particles generate in the carrier phase turbulence as fluid is deflected around them, as shown for example by Lucci, Ferrante & Elghobashi (2010).

When we move from solid particles to liquid droplets as considered by Dodd & Ferrante (2016), new phenomena and parameters are introduced. One is the surface tension, σ between the droplets and carrier fluid while another is the ratio of the dynamic viscosities of the dispersed and carrier fluids, $\gamma = \mu_d/\mu_c$. A liquid droplet can deform due to variations in pressure and normal viscous stresses across the droplet surface. A representative scale for the pressure variations in a turbulent flow, at least for large scales, is $\rho_c U_{rms}^2$ where U_{rms} is the root-mean-square velocity fluctuation in the turbulence. So a gauge for the degree of deformation is the ratio of inertial pressure variations to the pressure difference given by the Young–Laplace relation, namely the Weber number $We_{rms} = \rho_c D U_{rms}^2/\sigma$. A droplet of diameter D will tend to remain spherical and so minimize the interfacial surface energy if $We_{rms} \ll 1$. If the viscosity ratio γ is large the circulation inside a droplet is limited. Both of these conditions would apply to a 50 μm water droplet in an atmospheric cloud, where it is effectively a rigid particle. The story is different though for larger droplets or in liquid–liquid flows.

Droplets do not just deform but can breakup or coalesce with another drop, so changing the topology and the number of droplets involved. Atomization of a liquid jet with a coaxial gas stream will rapidly generate a fine spray of droplets with a range of sizes depending on the Reynolds number of the flow and the Weber number (Lasheras & Hopfinger 2000). Individual droplets in an air flow can undergo oscillations in shape and may fragment via different modes, again depending on We and γ (Flock *et al.* 2012). These features are included in engineering models and correlations but there is still limited information from first-principles direct numerical simulations. Such simulations are important as they can address questions not easily accessible in currently available experiments. It is against this background that the present paper presents a new perspective.

2. Overview

Dodd & Ferrante (2016), hereafter DF, explore the dynamics of liquid droplets added to an isotropic turbulent flow and they specifically go beyond the context of neutrally buoyant droplets. Isotropic turbulence is chosen as representative of the mid-range and small scales of most high Reynolds number turbulent flows and it has been the basis of many prior numerical simulations of dispersed two-phase flow. The large eddies in the base flow are characterized by the integral length scale l of the velocity fluctuations and there is the intermediate Taylor microscale λ, which here is close to $20\eta_K$. There is no forcing of the flow so as to avoid possible spurious correlations of the droplet dynamics, and so the turbulence decays over time. The flow is allowed to develop first before the droplets are introduced, at which point the Reynolds number $Re_\lambda = U_{rms}\lambda/\nu = 83$. As the turbulence decays over the period of the simulations, $t = 1$ to $t = 6$, Re_λ drops to 54, for the base flow without droplets and the mean turbulent kinetic energy k drops by 60 %.

DF consider a range of parameter values for We_{rms}, φ, γ but here we will just comment on cases B–D from DF where $We_{rms} = 0.1, 1, 5$ and the droplets are denser

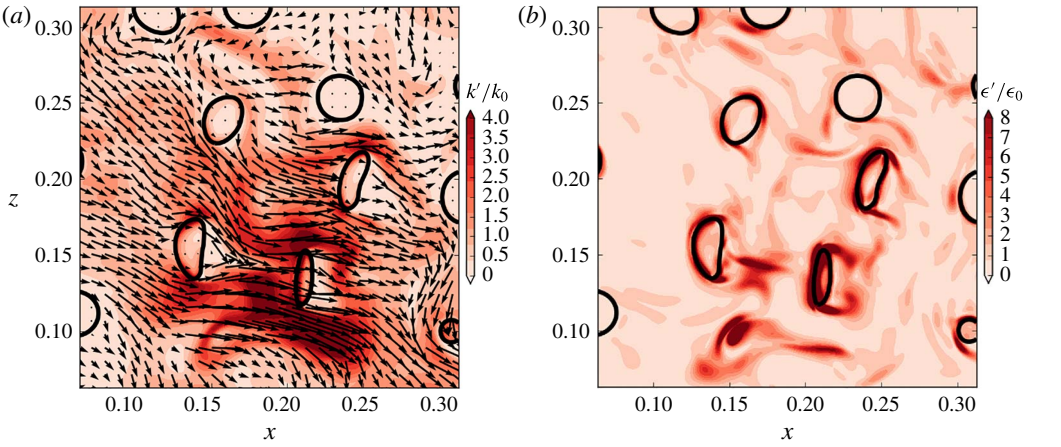

FIGURE 1. Results from Dodd & Ferrante (2016) for a planar section of a subregion of the flow at $t = 1.5$ showing the droplets for case C with $We_{rms} = 1$, $\varphi = 10$ and $\mu_d/\mu_c = 10$. In (*a*) contours of turbulent kinetic energy are shown with the black arrows giving the instantaneous velocity vectors projected onto the plane, as shown in figure 8(*b*) of DF. In (*b*), the corresponding contours are shown for the instantaneous local rate of viscous dissipation ϵ' as given in figure 11(*b*) of DF.

($\varphi = 10$) and more viscous ($\gamma = 10$) than the carrier fluid. In all cases, the droplet volume fraction is $\phi_v = 5\,\%$ and for this set of cases the mass fraction is 34 %. When the droplets are added to the flow, they are spherical with no internal circulation and their diameter D is set to be $20\eta_K$. DF use a form of immersed interface method with a fixed numerical mesh and a volume of fluid scheme, taking care in evaluating the forces due to surface tension, the droplet shape and handling the rapid changes in fluid density and viscosity across the droplet interface. Fuster *et al.* (2009) describe the technical challenges of computing these two-phase flows.

Figure 1 shows a sample of the droplets for case C from DF, $We_{rms} = 1$, soon after they are introduced into the flow. The pressure and normal viscous stresses cause the droplets to flatten into almost spherical caps, while the tangential stresses generate an internal circulation in the droplets. As these droplets are inertial there is an initial adjustment as they acquire translational and angular momentum. A local disturbance flow forms around them producing net fluid forces and torques from the carrier phase which tends to align the droplets broadside to this flow. Beyond these forces and associated wakes there is a force dipole (stresslet) generated that would give rise to an effective Einstein viscosity in a dilute viscous suspension. Both factors enhance the local instantaneous viscous dissipation rate ϵ' near each droplet as illustrated by figure 1.

A key feature of DF is the analysis of the mean turbulent kinetic energy $k(t)$, as given in (3.6) and in more detail by the appendices of DF. Figure 5 of DF illustrates the partition of $k(t)$ between the continuous phase, k_c and droplet phase, k_d, together with the mean rate of conversion to internal energy by viscous dissipation in each phase, $\epsilon = \epsilon_c + \epsilon_d$. A significant amount of energy is stored as interfacial surface energy and the power of surface tension Ψ_σ is defined as the rate of work by surface tension forces, being positive as the total surface area of the droplets decreases. The rate of increase of kinetic energy $k(t)$ is $-\epsilon + \Psi_\sigma$. The initial droplet deformation which increases the interfacial area actually represents a small energy loss compared to viscous dissipation ϵ as shown in figure 10 of DF. More significant is the droplet

coalescence that occurs later on. In cases B and C ($We_{rms} = 0.1,\ 1$), the total number of droplets and the interfacial area decrease steadily as the droplets collide and eventually coalesce. The effect is more pronounced for case B, where σ is ten times greater than for case C, and Ψ_σ becomes an appreciable source of energy. Droplets continue to coalesce forming increasingly larger ones as indicated by figure 17 of DF.

The deformation of droplets is not steady and they undergo shape oscillations excited by the turbulent fluctuations. These tend to be damped by viscosity which can add to the total dissipation ϵ. They also influence the rate of droplet coalescence, which depends on both near contacts of droplets and the drainage of the intervening fluid film. Shape oscillations and deformation contribute to breakup of the droplets, as seen for both cases D and F. For case D, $We_{rms} = 5$, the authors observe flattened droplets and thin ligaments forming at the edges that then exhibit a Rayleigh instability and shed several small droplets.

Beyond these physical observations, DF provides an in-depth analysis of the energy budgets for both the carrier phase and the droplets, separately accounting for pressure $T_{p,c}$, $T_{p,d}$ and viscous stresses $T_{v,c}$, $T_{v,d}$. These control the exchange of kinetic energy between the phases and taken together balance Ψ_σ, as in (3.12). The analysis is a new level of detail that gives insight into the links between interfacial surface energy and the turbulence.

3. Future

Continuing advances in methods for large-scale simulations with better control of mass conservation, adaptive refinement and the ability to handle large density and viscosity ratios are making it feasible to explore more deeply the dynamics of turbulent liquid–liquid or liquid–gas disperse two-phase flow. The work of DF is significant in terms of the large number of droplets, 3130 initially, and resolution ($D = 32\Delta x$) which makes meaningful statistical analysis possible. Many questions remain open for both droplet and bubble flows. One of these is the evolution of the droplet spectrum and the observation by Lasheras & Hopfinger (2000) that in a stationary flow a balance between breakup and coalescence results in an equilibrium size distribution independent of the initial spectrum. The experiments by Bateson & Aliseda (2012) address this for small droplets ($D \leqslant \eta_K$) at very low volume fractions for conditions relevant to atmospheric clouds. It remains to be seen what happens in more general engineering (and culinary) contexts.

References

Balachandar, S. & Eaton, J. K. 2010 Turbulent dispersed multiphase flow. *Annu. Rev. Fluid Mech.* **42**, 111–133.

Bateson, C. P. & Aliseda, A. 2012 Wind tunnel measurements of the preferential concentration of inertial droplets in homogeneous isotropic turbulence. *Exp. Fluids* **52**, 1373–1387.

Dodd, M. S. & Ferrante, A. 2016 On the interactions of Taylor lengthscale size droplets and isotropic turbulence. *J. Fluid Mech.* **806**, 356–412.

Flock, A. K., Guildenbecher, D. R., Chen, J., Sojka, P. E. & Bauer, H.-J. 2012 Experimental statistics of droplet trajectory and air flow during aerodynamic fragmentation of liquid drops. *Intl J. Multiphase Flow* **47**, 37–49.

Fuster, D., Agbaglah, G., Josserand, C., Popinet, S. & Zaleski, S. 2009 Numerical simulation of droplets, bubbles and waves: state of the art. *Fluid Dyn. Res.* **41** (6), 065001.

Lasheras, J. C. & Hopfinger, E. J. 2000 Liquid jet instability and atomization in a coaxial gas stream. *Annu. Rev. Fluid Mech.* **32**, 275–308.

Lucci, F., Ferrante, A. & Elghobashi, S. 2010 Modulation of isotropic turbulence by particles of Taylor length-scale size. *J. Fluid Mech.* **650**, 5–55.